INTERACTION BETWEEN P22^{PHOX} AND NOX4 IN THE ENDOPLASMIC RETICULUM SUGGESTS A UNIQUE MECHANISM OF NADPH OXIDASE COMPLEX FORMATION

Melinda Zana[1,2], Zalán Péterfi[1], Hajnal A. Kovács[1,2], Zsuzsanna E. Tóth[3], Balázs Enyedi[1], Françoise Morel[4], Marie-Hélène Paclet[4], Ágnes Donkó[1,2], Stanislas Morand[5Π], Thomas L. Leto[5] and Miklós Geiszt[1,2,*]

[1]Department of Physiology, Faculty of Medicine, Semmelweis University, Budapest, Hungary

[2]"Momentum" Peroxidase Enzyme Research Group of the Semmelweis University and the Hungarian Academy of Sciences, Budapest, Hungary

[3]Department of Anatomy, Histology and Embryology, Semmelweis University, Budapest, Hungary

[4]GREPI AGIM FRE CNRS 3405, Joseph Fourier University Grenoble France, EFS Rhône-Alpes

[5]Laboratory of Host Defenses, NIAID, NIH

[Π] Present address: L'Oreal Biotechnologies Research Laboratory, Aulnay-Sous-Bois, France

*Corresponding author: Miklós Geiszt

Department of Physiology, Semmelweis University, Faculty of Medicine, PO Box 259

H-1444 Budapest, Hungary

Telephone: 36-1-459-1500 ext: 60415 Fax: 36-1-266-7480

e-mail: geiszt.miklos@med.semmelweis-univ.hu

ABSTRACT

The $p22^{phox}$ protein is an essential component of the phagocytic- and inner ear NADPH oxidases but its relationship to other Nox proteins is less clear. We have studied the role of $p22^{phox}$ in the TGF-β1-stimulated H_2O_2 production of primary human and murine fibroblasts. TGF-β1 induced H_2O_2 release of the examined cells, and the response was dependent on the expression of both Nox4 and $p22^{phox}$. Interestingly, the $p22^{phox}$ protein was present in the absence of any detectable Nox/Duox expression, and the $p22^{phox}$ level was unaffected by TGF-β1. On the other hand, Nox4 expression was dependent on the presence of $p22^{phox}$, establishing an asymmetrical relationship between the two proteins. Nox4 and $p22^{phox}$ proteins localized to the endoplasmic reticulum and their distribution was unaffected by TGF-β1. We used a chemically induced protein dimerization method to study the orientation of $p22^{phox}$ and Nox4 in the endoplasmic reticulum membrane. This technique is based on the rapamycin-mediated heterodimerization of the mammalian FRB domain with the FK506 binding protein. The results of these experiments suggest that the enzyme complex produces H_2O_2 into the lumen of the endoplasmic reticulum, indicating that Nox4 contributes to the development of the oxidative milieu within this organelle.

KEYWORDS : Reactive oxygen species / NADPH oxidase / Nox4 / Hydrogen peroxide / $p22^{phox}$

ABBREVIATIONS:

Nox4: NADPH oxidase 4
Nox2: NADPH oxidase 2
Duox: dual oxidase
TGF-β1: transforming growth factor β1
ROS: reactive oxygen species
HPF: human pulmonary fibroblast
TTF: tail-tip fibroblast
FKBP: FK506 binding protein
ERO1: ER oxidoreductin 1

INTRODUCTION

Regulated production of reactive oxygen species (ROS) is now considered an essential component of maintaining homeostasis of live organisms [22,29]. Among ROS, hydrogen peroxide (H_2O_2) has emerged as a particularly important molecule with pleiotropic functions that include roles in host defense, thyroid hormone production, synthesis of the extracellular matrix and signal transduction[22]. H_2O_2 is produced at different intracellular sites as a byproduct of various biochemical pathways, but regulated production of H_2O_2 is mediated by members of the Nox/Duox family of NADPH oxidases[16,22]. Nox2, the prototypic enzyme of this family, was originally identified in phagocytes, whereas non-phagocytic Nox/Duox isoforms are expressed and function in a wide variety of cells and tissues.

Currently, the most intensively studied, dedicated ROS source is Nox4, which was originally identified in kidney epithelial cells[15,33]. Subsequent studies revealed that the expression of Nox4 is not restricted to the kidney, but other cells including endothelial and alveolar epithelial cells, osteoclasts, cardiomyocytes and activated fibroblasts also contain the enzyme[3]. The physiological function of Nox4 remains unclear. Recent studies on knockout animals suggest that ROS production by Nox4 is often protective in different disease models[31,42], although pathogenic roles were also described for the enzyme[18,20].

We know little about the regulation of Nox4. Several data suggest that the activity of Nox4 is regulated at the transcriptional level[7], but acute, hitherto unknown regulatory mechanisms might also exist. Nox/Duox proteins often interact with other partners to form fully active enzyme complexes[7]. Genetic evidence proves that $p22^{phox}$, which was originally identified as a component of the phagocytic oxidase, also supports the biological activity of Nox3[25]. Furthermore, in heterologous expression systems, the activity of both Nox4 and Nox1 was stimulated by the co-expression of $p22^{phox}$[1] [19,24]. In the majority of the Nox4-related studies, the activity and localization of the enzyme were analyzed in heterologous expression systems. However, it remained unknown, whether the activity of Nox4 is also dependent on $p22^{phox}$ in cells where these proteins are naturally co-expressed. Using genetically-modified cell models we demonstrate that endogenously expressed $p22^{phox}$ is an essential component of the Nox4 enzyme complex, and we demonstrate an asymmetrical relationship between the two proteins: the level of $p22^{phox}$ is not influenced by Nox4 expression; however the stability of Nox4 is dependent on the presence of $p22^{phox}$. We also show that the Nox4-$p22^{phox}$ complex localizes to the endoplasmic reticulum, and their membrane topology is compatible with ROS being released into the lumen of the endoplasmic reticulum.

EXPERIMENTAL PROCEDURES

Materials

The Alexa488 and 568-labeled goat monoclonal anti-mouse and polyclonal anti-rabbit Fab-antibodies were obtained from Life Technologies. The monoclonal anti-V5 antibody was purchased from AbD Serotec. The 16G7, IgG1-type monoclonal anti-$p22^{phox}$ antibody was previously characterized by the authors[8]. The monoclonal anti-AU1 was obtained from Covance (AFC-130P), while the rabbit polyclonal was ordered from Abcam (ab3401). The monoclonal β-actin and all other chemicals were purchased from Sigma-Aldrich unless otherwise stated. Rapamycin was a kind gift of Péter Várnai. The anti-Nox4 antibody was obtained from Novus Biologicals.

Cell culture

Hela wt (ATCC: CCL-2™), dermal fibroblast (BJ, ATCC: CRL-2522™) and HEK293 FS cells were grown in DMEM (Lonza) supplemented with 10% fetal bovine serum (FBS), 50 U/mL penicillin and 50 μg/mL streptomycin (Sigma-Aldrich). Human pulmonary fibroblasts (HPF, PromoCell, C-12360) were grown in fibroblast medium (PromoCell) supplemented with 2% FBS, 5 ng/mL Basic Fibroblast Growth Factor and 5 μg/mL insulin. Nox4-overexpressing HEK 293 FS cells were described in our previous report[12]. The fibroblasts of $p22^{phox}$-mutant *(nmf333)*[25] and Nox4 knockout (3FAFyh) mice were generated from tail tips of 8-weeks-old animals. After 30 min collagenase digestion of the tail tips, cells were cultured in DMEM containing 10% FBS and 1% penicillin/streptomycin for several days. Before TGF-β1 treatment, we serum.deprived the cells in the presence of 0.05% serum. Cells were treated with TGF-β1 (R&D Systems, Minneapolis, MN) for 24 h in the absence of serum.

Animals

Nox4-deficient mice (strain 3FAFyh), obtained from the Biology Division of the Oak Ridge National Laboratory (Oak Ridge, TN), were identified within a group of homozygous-viable, radiation-induced albino mice that lack the *Tyrosinase* (*Tyr*) color coat gene[30]. *Nox4* and *Tyr* are adjacent gene sequences located on the q-arm (c-locus) of chromosome 7. Southern blots probed with the full-length Nox4 cDNA confirmed the absence of the entire *Nox4* genomic sequence. PCR-based analysis was used to determine the boundaries of the mutated *Nox4-Tyr* locus, which revealed a deletion ~2100 kilobases in length. Most of the deleted segment encompassed a region upstream of Nox4 that includes a cluster of olfactory-vomeronasal receptor genes and pseudogenes (*Vmn2r-70* through *Vmn2r-79*) and folate hydrolase (*Folh1*), followed by *Nox4* and *Tyr*. Intact *Gmr5* and *Ctsc* genomic sequences were detected immediately distal to this deleted sequence.

$p22^{phox}$-mutant *(nmf333)* mice were obtained from The Jackson Laboratory (Bar Harbor, ME). Animals were maintained on a standard diet and given water ad libitum.

DNA constructs and transfection

The $p22^{phox}$-containing plasmids were generated by PCR based amplification of $p22^{phox}$ ORF from human renal cDNA (Applied Biosystems/Ambion, Austin, TX, USA) with a forward primer pair containing a 5' NheI and 3' BamHI sites followed by a V5-epitope-encoding sequence to frame into pcDNA3.1 vector. The $p22^{phox}$-AU1 epitope-tagged version was created with site-directed mutagenesis (QuikChange II Site-Directed Mutagenesis Kit, Agilent) by using primers containing the AU1-coding sequence. The V5-tagged Nox4 pcDNA3.1 plasmid was available in our lab, and it was used for further modification with different tags. N-terminal AU1 tag was introduced by site-directed mutagenesis. CFP-FRB-HA-tag was amplified with NheI-BglII restriction sites by PCR from a pEGFP-based vector of P. Várnai [37] and ligated to the N-terminal site of Nox4. The $p22^{phox}$-FRB-HA-CFP was generated by PCR amplification from the previous vector, with SalI-MfeI restriction sites to ligate into the C-terminal end of $p22^{phox}$. The FRB-YFP plasmid was received from P. Várnai's lab[37].

Vectors encoding HyPer (cytosolic) described by Belousov et al.[4] were purchased from Evrogen (Moscow, Russia). The targeted versions of HyPer were formerly cloned and described by Enyedi *et al.*[13]. All constructs have been verified by DNA sequencing.

Plasmids were transfected by using Lipofectamine LTX (Life Technologies) or with Neon Transfection System (Life Technologies) in the stage of 60-70% confluency. For gene silencing we applied standard siRNA treatment: we transfected 60-80% confluent, adherent cells with 25 pM specific or scrambled siRNA with Lipofectamine RNAiMAX (Life Technologies) according to the manufacturer's instructions. After transfection, the cells were incubated for further 2-3 days.

Immunocytochemistry

Cells were plated on coverslips were fixed in 4% paraformaldehyde in PBS, and then washed and quenched for 10 min in 100 mM glycine in PBS. After four times washing in PBS, cells were permeabilized in 1% BSA and 0.1% Triton X-100 in PBS for 20 min. We blocked the cells for 1 hour in 3% BSA in PBS. Cells were subsequently incubated with primary antibody in 3% BSA-containing PBS for 1 or 2 hours, then washed in PBS several times. The secondary antibody was used for 1 hour in 3% BSA in PBS then washed in PBS again. After the final washing steps the cells were mounted with Mowiol 4–88 antifade reagent [Tris (pH 8.5) and glycerol-based polyvinyl alcohol 4–88].

Western blot analysis

In Western Blot experiments, cells were washed once with cold PBS, then lysed in RIPA buffer (50 mM Tris, 150 mM NaCl, 0.1% SDS, 0.5% Na-deoxycholate, 1% Triton-X) enriched with proteinase

inhibitor cocktail (Roche Life Science) then were spun at 13400 rpm for 10 min. After that, the supernatant was combined with 4×Laemmli sample buffer [0.005% Bromophenol blue, 4% SDS, 20% glycerol, 0.1 M Tris (pH 6.8)] then loaded without boiling on 12% SDS–polyacrylamide gels. After electrophoresis, the gels were blotted onto nitrocellulose membranes, blocked in 5% milk powder containing PBS for 1 hour or overnight. The primary antibody was incubated for 1 hour in 3% BSA-containing PBS at room temperature. The binding was visualized by peroxidase-coupled goat anti-mouse or anti-rabbit IgG (GE Healthcare), using the enhanced chemiluminescence method (Millipore).

Fluorescent intensity measurements and confocal microscopy

Immunostained cell images were collected on a Zeiss LSM710 confocal laser scanning microscope equipped with a 63x1.4 oil immersion numerical aperture plan Apochromat objective (Zeiss). Images were acquired from optical slices of 1–2 μm thickness. Alexa488 immunofluorescence detection involved excitation with a 488 nm argon laser, while in case of Alexa568 the 543 nm helium/neon laser was applied. Emissions were collected using a 500-530 nm band-pass filter and Alexa488 and a 560 nm long-pass filter for Alexa568. Image analysis was performed using Zen software (Zeiss).The ratiometric measurements of HyPer were performed on an inverted microscope (Axio Observer, Zeiss) equipped with 40x1.4 oil-immersion objective (Fluar, Zeiss) and a Cascade II. camera (Photometrics, Tucson, AZ). Excitation wavelengths were set by a random-access monochromator connected to a xenon arc lamp (DeltaRAM, Photon Technology International, Birmingham, NJ). The excitation wavelengths of HyPer are 490 and 420 nm combined with a 505 nm dichroic filter and a 525/36 nm emission filter set. Data acquisition was handled by Metafluor software (Molecular Devices, Downingtown, PA). Ratios were calculated upon background fluorescence subtraction. We applied FKBP12-FRB system as a chemically inducible translocation assay with rapamycin as an inducer. Within a cell, after administration of 300nM rapamycin, the molecule first binds to FKBP12 (12-kDa FK506-binding protein) and only then the FKBP12–rapamycin complex binds to FBR, which is the FKBP and rapamycin binding domain of TOR kinase[28,37]. BJ fibroblasts were plated in six-well dishes at 60% confluence and cotransfected the CFP-FKBP12-Nox4 or p22phox-FKBP12-CFP with FRB-YFP together with electroporation. Kinetic measurements were performed at cell chamber (AttoFluor, Life Technologies) containing coverslips at room temperature in 1 ml HEPES-buffered medium (H-medium), where stimuli were added in 0.1 ml of H-medium. Images were acquired every 5-10 seconds for a period of 15 min.

In situ hybridization

Animals were sacrificed by decapitation, the kidneys were removed and frozen on dry ice. 12 μm-thick sections were cut in a cryostat (Leica Microsystems GmbH, Wetzlar, Germany) and mounted onto

positively charged Superfrost Plus slides (Life Technologies Magyarország Kft, Budapest, Hungary). To create templates for probe synthesis, the full coding sequence of the mouse $p22^{phox}$ cDNA and a DNA fragment composed of the last 300 bps of the murine Nox4 coding sequence were subcloned into PCR 4.0 TOPO vector (Life Technologies). Hybridizations were performed with 10^6 cpm/slide of the [35S]UTP-labeled (Per-Form Hungaria Kft, Budapest, Hungary) antisense and sense riboprobes, prepared according to the MAXIscriptT7/T3 Transcription Kit (Life Technologies), overnight at 55°C. Next day the slides were washed, dehydrated and dipped into NTB nuclear track emulsion (Carestream Health Deutschland GmbH, Stuttgart, Germany) for 3 days. Emulsion-coated slides were developed using Kodak Dektol developer and Fixer (Sigma-Aldrich Kft, Budapest, Hungary). Sections were counter-stained with 0.5% Giemsa solution (Sigma), air dried and coverslipped using Cytoseal 60 mounting medium (Stephens Scientific, Riverdale, NJ, USA).

Amplex Red assay for extracellular H_2O_2 level quantification

The extracellular H_2O_2 levels were measured with Amplex Red method (Life Technologies). Adherent confluent cells were incubated in the presence of 50μM Amplex red and 0.1 U/ml horseradish peroxidase in H-medium. After 40 min incubation at 37°C, resorufin fluorescence was measured at 590 nm.

Statistics

Data are presented as mean ± S.E.M unless otherwise stated. Statistical analyses were performed using Sigmaplot 13.0 software for Windows (Systat Software Inc.). For estimating the significance of differences Student's t-test or Mann-Whitney-U test was used.

RESULTS

TGF-β1-induced H_2O_2 production of primary fibroblasts is dependent on Nox4- and $p22^{phox}$ expression

Since TGF-β1 was described to stimulate Nox4-dependent H_2O_2 production [23] and this response seems to have multiple roles in TGF-β1 signaling [9] [6,10], we decided to study the role of $p22^{phox}$ in primary human and mouse fibroblasts stimulated by TGF-β1. As shown in Fig. 1, treatment of human pulmonary (HPF) or foreskin-derived (BJ) fibroblasts with TGF-β1 for 24 h lead to increased H_2O_2 production. Experiments using Nox4-specific siRNAs confirmed that Nox4 was responsible for the increased ROS output (Figs. 1A and 1B).

The participation of Nox4 in TGF-β1-stimulated H_2O_2 release has not yet been confirmed by experiment on gene-deficient cells, thus we prepared tail-tip fibroblasts (TTFs) form Nox4 knockout and wild-type animals and studied the effect of TGF-β1 on the H_2O_2 output of the cells. TGF-β1 effectively stimulated the H_2O_2 production of wild-type cells, but Nox4-deficient fibroblasts failed to exhibit enhanced ROS production (Fig. 2A). This result clearly suggested the essential role of Nox4 in the ROS response. Next, we wanted to assess the importance of $p22^{phox}$ in the TGF-β1-stimulated H_2O_2 response. To achieve this, we prepared TTFs from the *nmf333 strain* mice that carry a mutation in the *CYBA* gene[25], leading to instability of the encoded protein. This mutation was described to result in a decreased Nox2-mediated ROS production in neutrophil granulocytes[25]. Fig. 2B shows that TGF-β1-treated $p22^{phox}$-deficient TTFs released significantly less H_2O_2 than cells prepared from wild-type littermates. This experiment proved that endogenously expressed $p22^{phox}$ supports the activity of Nox4.

The expression of $p22^{phox}$ in primary fibroblasts is independent of Nox4

According to our current understanding, Nox4 is mainly regulated at the level of gene transcription, and the stimulatory effect of TGF-β1 is a consequence of increased Nox4 expression[7]. We wanted to know, whether TGF-β1 also stimulates the expression of $p22^{phox}$ that proved to be an essential partner of Nox4 in previous experiments. After exposure to TGF-β1 for 24 h, we observed the induction of Nox4 mRNA expression in both HPFs and BJ fibroblasts (Fig. 3A). Interestingly, the expression of $p22^{phox}$ mRNA in the same cell types was unaffected by TGF-β1 (Fig. 3A). In further experiments, we analyzed the $p22^{phox}$ protein content of control- and TGF-β1-stimulated HPFs and BJ fibroblasts. These experiments revealed that the $p22^{phox}$ protein is already expressed in unstimulated cells, and its level remains constant following TGF-β1 treatment (Fig. 3B). We also studied $p22^{phox}$ expression levels in a cell line where Nox4 was heterologously expressed [12]. Fig. 3C (right panel) shows a marked increase in H_2O_2 production by Nox4-expressing cells, whereas the $p22^{phox}$ content of the Nox4-expressing and parent cell line was essentially the same (Fig. 3C, left panel). In subsequent experiments, we compared the $p22^{phox}$ expression of wild-type and Nox4-deficient TTFs. As shown in Fig. 3D, the $p22^{phox}$ protein was present in the genetic absence of Nox4 and its level was unaffected by TGF-β1. Altogether, the results of the above-described experiments suggested that the expression of $p22^{phox}$ is independent of Nox4, and complex formation with Nox4 is not required for $p22^{phox}$ stabilization.

Nox4 is stabilized by $p22^{phox}$ in the kidney

Next, we wanted to examine whether the presence of $p22^{phox}$ is required for the expression of the Nox4 protein or it regulates Nox4 activity by other means. Since we could not detect Nox4 at the protein level in TGF-β1-stimulated fibroblasts, we decided to study the interaction between the two proteins in the kidney that shows the highest Nox4 level among mammalian organs[15]. First, we checked whether Nox4 and $p22^{phox}$ are expressed in the same region of the kidney. *In situ* hybridization experiments confirmed that Nox4 and $p22^{phox}$ mRNAs are both present in proximal tubules epithelial cells (Figs. 4A-D). Next, we studied the $p22^{phox}$ content of kidney lysates from wild-type, $p22^{phox}$ mutant (*nmf333*) and Nox4-deficient animals. As shown in Fig. 4E the level of $p22^{phox}$ was unaffected in the absence of Nox4, whereas $p22^{phox}$ mutation resulted in reduced protein level. When the expression of Nox4 was analyzed in the same samples we found Nox4 to be absent in both $p22^{phox}$ mutant and Nox4-deficient kidney lysates (Fig. 4F). This observation suggests that $p22^{phox}$ is essential for the stabilization of Nox4 in kidney epithelial cells.

Nox4 and $p22^{phox}$ localize to the endoplasmic reticulum of primary fibroblasts

Since our previous experiments revealed an intimate relationship between $p22^{phox}$ and Nox4, we wanted to determine the intracellular localization of $p22^{phox}$ in primary fibroblasts. Unfortunately, none of the tested $p22^{phox}$-specific antibodies gave specific labeling; thus, we added a V5 epitope to the C-terminus of $p22^{phox}$ and studied the distribution of the labeled protein. Fig. 5A shows that $p22^{phox}$-V5 localized to the endoplasmic reticulum in BJ fibroblasts. This staining pattern was not due to the modification of the C-terminal part of $p22^{phox}$ since introducing a different (AU1) tag into the protein did not change the characteristic localization pattern (data not shown). As we demonstrated in earlier experiments, Nox4 was absent in unstimulated primary fibroblasts. Therefore, it was possible that localization of $p22^{phox}$ to the ER did not represent the final position of the protein in the Nox4 enzyme complex. We, therefore, tested whether the subcellular distribution of $p22^{phox}$ changes upon TGF-β1 stimulation, e.g. under conditions when Nox4 becomes induced. As shown in Fig. 5A, TGF-β1 treatment did not modify the localization of $p22^{phox}$ that remained in the endoplasmic reticulum. When an epitope-labeled version Nox4 was introduced into fibroblasts by heterologous expression, it was also detected in the ER, where it co-localized with BiP (Fig. 5B). These observations suggested that the physiological location of the $p22^{hox}$-Nox4 complex in primary fibroblasts is the ER.

Orientation of $p22^{phox}$ and Nox4 in the endoplasmic reticulum membrane

H_2O_2 production by Nox4 in TGF-β1-stimulated fibroblasts is readily detected in the extracellular space, although the enzyme complex localizes to an intracellular compartment. We, therefore, became interested

in determining the orientation of the Nox4-$p22^{phox}$ complex in the ER membrane. To study the orientation of $p22^{phox}$, we applied a chemically induced protein dimerization technique, which is based on the rapamycin-induced heterodimerization of the mammalian FRB domain with the FK506 binding protein[28,37]. We coupled FRB along with the Cyan Fluorescent Protein (CFP) to the C-terminus of $p22^{phox}$ and FKB12 was labeled with the Yellow Fluorescent Protein (YFP). Fig. 6A shows that the FRB-CFP labeled $p22^{phox}$ localized to the ER, whereas the FKB12-YFP protein was cytosolic (Fig. 6B). After the addition of rapamycin the FKB12-YFP protein rapidly relocated to the ER indicating that the dimerization event occurred on the cytosolic surface of the ER (Fig. 6D). In other experiments, we introduced the FRB-CFP tag to N-terminus of Nox4. This Nox construct also located to ER and following the addition of rapamycin, the YFP-linked FKBP12 showed colocalization with Nox4 (Fig. 6H). Based on these experiments, the orientations of $p22^{phox}$ and Nox4 are compatible with ROS release into the lumen of the endoplasmic reticulum (Figs. 6I and J).

DISCUSSION

Nox4 is currently the most intensively studied regulated source of hydrogen peroxide. Although Nox4 was originally identified in the kidney [15,33], Nox4-dependent production of ROS is now recognized in several other tissues and cells. The great majority of Nox4-related studies aimed to identify the physiological and pathological roles of Nox4-derived H_2O_2. Thus, we still know little about the protein interactions and regulation of Nox4 [7,34]. The intracellular localization of Nox4 is also obscure since the enzyme was detected at several different intracellular locations [5,17,21,39,41].

In this work, we characterized the expression and function of $p22^{phox}$ in primary fibroblasts and kidney, i.e. at locations where Nox4 is also endogenously expressed. Our experiments revealed an interesting asymmetrical relationship between $p22^{phox}$ and Nox4. We found $p22^{phox}$ to be expressed in the absence of Nox4 in both fibroblasts and the kidney, but the presence of $p22^{phox}$ was required for the activity of Nox4. Since Nox4 protein was not detected in kidney lysates of $p22^{phox}$ mutant animals, we can conclude that $p22^{phox}$ is required for the stabilization of Nox4.

$p22^{phox}$ was first identified as an essential membrane component of the phagocytic oxidase, where together with Nox2 they form the cytochrome b_{558} complex[26,32]. According to our current view of the phagocytic oxidase, cytochrome b_{558} catalyzes the final steps of electron transfer during superoxide production. $P22^{phox}$ was also described as an essential component of an NADPH oxidase expressed in vascular smooth muscle cells, but the identity of the partner Nox isoform was unknown at the time [36]. Genetic evidence supports the cooperation between $p22^{phox}$ and Nox3, as mice with a mutant $p22^{phox}$ gene

exhibit a vestibular defect that is similar to the one observed in Nox3-deficient animals[25]. In heterologous expression models, $p22^{phox}$ was also found to interact with and support the activity of Nox4[1,24] [19], however, our data obtained from experiments on $p22^{phox}$-mutant fibroblasts provide genetic evidence for the importance of $p22^{phox}$ in the stabilization of endogenously expressed Nox4. The *nmf333* mutation results in a Y121H amino acid substitution in $p22^{phox}$[25]. When the effect of this amino acid change on Nox4 function was tested in a heterologous expression system, the stimulatory effect of the mutant $p22^{phox}$ protein was indistinguishable from the effect of its wild-type counterpart[38]. In a different study on Nox4-transfected HEK293 cells, the expression level of Nox4 was not affected by silencing $p22^{phox}$ [19]. The difference between these data and our results obtained from experiments on primary cells emphasizes the importance of cautious interpretation of data derived from heterologous expression systems.

In phagocytic cells, the presence of $p22^{phox}$ is essential for the stabilization of Nox2, and $p22^{phox}$ protein is detected only in the presence of Nox2, thus the simultaneous expression of both proteins is necessary for the appearance of the cytochrome b558 complex[27,35]. Stabilization of the $p22^{phox}$ protein by Nox4 was also reported in HEK293 cells transfected with epitope-tagged Nox4- and $p22^{phox}$ constructs [1]. However, several of our observations suggest that the symmetrical relationship between $p22^{phox}$ and Nox2 is not characteristic of the Nox4 system. First, we detected $p22^{phox}$ by Western blot in human pulmonary and foreskin fibroblasts that did not express any Nox proteins. TGF-β1 treatment of these cells boosted the expression of Nox4 and consequent ROS production, but the $p22^{phox}$ content of TGF-β1-treated cells did not differ from that of control, unstimulated cells. Furthermore, $p22^{phox}$ was also detected in Nox4-deficient TTFs, confirming that the presence of Nox4 is not required for the stabilization of $p22^{phox}$. It will be interesting to study whether this asymmetrical relationship between the two proteins is a unique feature of the Nox4 system or other Nox proteins (Nox1 and Nox3) behave similarly in cells where they are endogenously expressed.

It is noteworthy that we could not study the effect of $p22^{phox}$ on Nox4 expression in TGF-β1-stimulated fibroblasts because we were unable to detect Nox4 at the protein level in these cells. When we compared the $p22^{phox}$ content of primary fibroblasts and neutrophil granulocytes, we observed a much higher $p22^{phox}$ content in neutrophils than in fibroblasts (Fig. S1)**.** Since Nox proteins are supposed to form a 1:1 complex with $p22^{phox}$, the $p22^{phox}$ content of fibroblasts may limit the maximum of Nox4 expression. Apparently, this expression level is too low to be captured by anti-Nox4 antibodies which were tested during the course of our studies. This observation cautions for the critical interpretation of experiments where Nox4 is detected at the protein level by Western blot analysis.

The subcellular localization of Nox enzymes is one of the most important issues in the Nox/Duox research field. To know the specific intracellular sites of Noxes is critical because the highly reactive

species produced by these enzymes unlikely travel a long distance before exerting their effects; thus their intracellular localization is a major determinant of their affected targets[40]. In previous works Nox4 was detected at various intracellular locations including the plasma membrane, nucleus, mitochondria, endoplasmic reticulum, and focal adhesions [5,17,21,39,41]. It is possible that the subcellular distribution of Nox4 is cell type-specific, however, the lack of specific antibodies might also explain the observed differences. According to our results, $p22^{phox}$ resides in the endoplasmic reticulum of primary fibroblasts and this localization persists during myofibroblastic differentiation, e.g. when Nox4 becomes expressed in the cells. The localization of $p22^{phox}$ likely defines the site of the Nox4-$p22^{phox}$ complex, which in the case of TGF-β1-stimulated fibroblasts, appears to be the ER. Although we could not locate $p22^{phox}$ in the murine kidney by immunostaining, cell fractionation experiments suggest that protein – along with Nox4 – is enriched in the microsomal fraction of the cells (data not shown).

According to the current topological model of $p22^{phox}$, which was described in phagocytic cells, the protein has two transmembrane domains with both termini facing the cytosol. Our data obtained by rapamycin-induced dimerization technique suggests that $p22^{phox}$ resides in the ER membrane in a similar fashion, that is N- and C-termini located on the cytoplasmic side. This membrane topology would be compatible with H_2O_2 being released into the ER lumen. The ER lumen is characterized by a highly oxidative environment, which is probably due to the activity of the protein folding machinery. The oxidized state of the ER of primary fibroblasts was readily detected by an ER-targeted, redox-sensitive protein sensor, Hyper (data not shown). However, the already oxidized sensor would unlikely capture the presence of "extra" oxidants in the ER lumen. On the other hand, Nox4-derived H_2O_2 production by TGF-β1-activated cells was readily detected in the extracellular space, confirming earlier observations, where Nox4 was described to produce mainly H_2O_2 [11]. At the first sight, the localization of Nox4 in the ER does not seem to be compatible with ROS release to the extracellular space, however, the intimate relationship between the ER and the plasma membrane can explain the extracellular detection of Nox4-produced H_2O_2.

The function of Nox4 in TGF-β1-stimulated fibroblasts is still incompletely understood. In a previous study, where RNAi was used to suppress Nox4 activity, the enzyme was found to promote myofibroblastic differentiation [9]. On the other hand, experiments on Nox4 knockout mice did not support a role of Nox4 in the development of kidney fibrosis [2] and we did not observe altered fibroblast-myofibroblast transition in Nox4-deficient TTFs (data not shown). In more recent studies on vascular smooth muscle cells, Nox4 activity was found to have a role in TGF-β1-induced palladin expression [23] and focal adhesion formation [10]. This latter response seems to be dependent on the interaction of Hic-5 and HSP27, indicating a complex role for Nox4-derived ROS in the organization of cytoskeletal responses [14].

The formation and regulation of the redox environment in the ER is very complex and remains partially unexplored. According to our current understanding of the ER redox machinery, the major source of H_2O_2 in the ER is ERO1 which produces H_2O_2 during the oxidation of PDI. Thus, the production of H_2O_2 in the ER is essentially thought to be a byproduct of oxidative protein folding. The addition of a dedicated H_2O_2 source to this scene appears to indicate redundancy, however, the redox milieu of the ER is unlikely homogenous, and it is possible that different ROS sources are compartmentalized within the organelle. Hopefully, the future identification of Nox4 targets will improve our understanding of the Nox4-$p22^{phox}$ complex role in ER redox homeostasis.

ACKNOWLEDGMENTS

We are grateful to Beáta Molnár and Katalin Meczker for technical assistance. This work was supported by the Hungarian Research Fund (OTKA K106138 and K119955). This work was also supported by "Momentum" grant from the Hungarian Academy of Sciences.

CONFLICT OF INTEREST

The authors declare that they have no conflict of interest.

REFERENCES

[1] Ambasta, R. K.; Kumar, P.; Griendling, K. K.; Schmidt, H. H.; Busse, R.; Brandes, R. P. Direct interaction of the novel Nox proteins with p22phox is required for the formation of a functionally active NADPH oxidase. *J. Biol. Chem.* **279**:45935-45941; 2004.

[2] Babelova, A.; Avaniadi, D.; Jung, O.; Fork, C.; Beckmann, J.; Kosowski, J.; Weissmann, N.; Anilkumar, N.; Shah, A. M.; Schaefer, L.; Schroder, K.; Brandes, R. P. Role of Nox4 in murine models of kidney disease. *Free Radic. Biol. Med.* **53**:842-853; 2012.

[3] Bedard, K.; Krause, K. H. The NOX family of ROS-generating NADPH oxidases: physiology and pathophysiology. *Physiol Rev.* **87**:245-313; 2007.

[4] Belousov, V. V.; Fradkov, A. F.; Lukyanov, K. A.; Staroverov, D. B.; Shakhbazov, K. S.; Terskikh, A. V.; Lukyanov, S. Genetically encoded fluorescent indicator for intracellular hydrogen peroxide. *Nat. Methods* **3**:281-286; 2006.

[5] Block, K.; Gorin, Y.; Abboud, H. E. Subcellular localization of Nox4 and regulation in diabetes. *Proc. Natl. Acad. Sci. U. S. A* **106**:14385-14390; 2009.

[6] Boudreau, H. E.; Casterline, B. W.; Rada, B.; Korzeniowska, A.; Leto, T. L. Nox4 involvement in TGF-beta and SMAD3-driven induction of the epithelial-to-mesenchymal transition and migration of breast epithelial cells. *Free Radic. Biol. Med.* **53**:1489-1499; 2012.

[7] Brandes, R. P.; Weissmann, N.; Schroder, K. Nox family NADPH oxidases: Molecular mechanisms of activation. *Free Radic. Biol. Med.* **76C**:208-226; 2014.

[8] Campion, Y.; Jesaitis, A. J.; Nguyen, M. V.; Grichine, A.; Herenger, Y.; Baillet, A.; Berthier, S.; Morel, F.; Paclet, M. H. New p22-phox monoclonal antibodies: identification of a conformational probe for cytochrome b 558. *J. Innate. Immun.* **1**:556-569; 2009.

[9] Cucoranu, I.; Clempus, R.; Dikalova, A.; Phelan, P. J.; Ariyan, S.; Dikalov, S.; Sorescu, D. NAD(P)H oxidase 4 mediates transforming growth factor-beta1-induced differentiation of cardiac fibroblasts into myofibroblasts. *Circ. Res.* **97**:900-907; 2005.

[10] Datla, S. R.; McGrail, D. J.; Vukelic, S.; Huff, L. P.; Lyle, A. N.; Pounkova, L.; Lee, M.; Seidel-Rogol, B.; Khalil, M. K.; Hilenski, L. L.; Terada, L. S.; Dawson, M. R.; Lassegue, B.; Griendling, K. K. Poldip2 controls vascular smooth muscle cell migration by regulating focal adhesion turnover and force polarization. *Am. J. Physiol Heart Circ. Physiol* **307**:H945-H957; 2014.

[11] Dikalov, S. I.; Dikalova, A. E.; Bikineyeva, A. T.; Schmidt, H. H.; Harrison, D. G.; Griendling, K. K. Distinct roles of Nox1 and Nox4 in basal and angiotensin II-stimulated superoxide and hydrogen peroxide production. *Free Radic. Biol. Med.* **45**:1340-1351; 2008.

[12] Donko, A.; Orient, A.; Szabo, P. T.; Nemeth, G.; Vantus, T.; Keri, G.; Orfi, L.; Hunyady, L.; Buday, L.; Geiszt, M. Detection of hydrogen peroxide by lactoperoxidase-mediated dityrosine formation. *Free Radic. Res.* **43**:440-445; 2009.

[13] Enyedi, B.; Varnai, P.; Geiszt, M. Redox State of the Endoplasmic Reticulum Is Controlled by Ero1L-alpha and Intraluminal Calcium. *Antioxid. Redox. Signal.* 2010.

[14] Fernandez, I.; Martin-Garrido, A.; Zhou, D. W.; Clempus, R. E.; Seidel-Rogol, B.; Valdivia, A.; Lassegue, B.; Garcia, A. J.; Griendling, K. K.; San Martin, A. Hic-5 Mediates TGFbeta-Induced Adhesion in Vascular Smooth Muscle Cells by a Nox4-Dependent Mechanism. *Arterioscler. Thromb. Vasc. Biol.* **35**:1198-1206; 2015.

[15] Geiszt, M.; Kopp, J. B.; Varnai, P.; Leto, T. L. Identification of renox, an NAD(P)H oxidase in kidney. *Proc. Natl. Acad. Sci. U. S. A* **97**:8010-8014; 2000.

[16] Geiszt, M.; Leto, T. L. The Nox family of NAD(P)H oxidases: host defense and beyond. *J. Biol. Chem.* **279**:51715-51718; 2004.

[17] Hilenski, L. L.; Clempus, R. E.; Quinn, M. T.; Lambeth, J. D.; Griendling, K. K. Distinct subcellular localizations of Nox1 and Nox4 in vascular smooth muscle cells. *Arterioscler. Thromb. Vasc. Biol.* **24**:677-683; 2004.

[18] Jha, J. C.; Gray, S. P.; Barit, D.; Okabe, J.; El Osta, A.; Namikoshi, T.; Thallas-Bonke, V.; Wingler, K.; Szyndralewiez, C.; Heitz, F.; Touyz, R. M.; Cooper, M. E.; Schmidt, H. H.; Jandeleit-Dahm, K. A. Genetic targeting or pharmacologic inhibition of NADPH oxidase nox4 provides renoprotection in long-term diabetic nephropathy. *J. Am. Soc. Nephrol.* **25**:1237-1254; 2014.

[19] Kawahara, T.; Ritsick, D.; Cheng, G.; Lambeth, J. D. Point mutations in the proline-rich region of p22phox are dominant inhibitors of Nox1- and Nox2-dependent reactive oxygen generation. *J. Biol. Chem.* **280**:31859-31869; 2005.

[20] Kuroda, J.; Ago, T.; Matsushima, S.; Zhai, P.; Schneider, M. D.; Sadoshima, J. NADPH oxidase 4 (Nox4) is a major source of oxidative stress in the failing heart. *Proc. Natl. Acad. Sci. U. S. A* **107**:15565-15570; 2010.

[21] Kuroda, J.; Nakagawa, K.; Yamasaki, T.; Nakamura, K.; Takeya, R.; Kuribayashi, F.; Imajoh-Ohmi, S.; Igarashi, K.; Shibata, Y.; Sueishi, K.; Sumimoto, H. The superoxide-producing NAD(P)H oxidase Nox4 in the nucleus of human vascular endothelial cells. *Genes Cells* **10**:1139-1151; 2005.

[22] Lambeth, J. D.; Neish, A. S. Nox enzymes and new thinking on reactive oxygen: a double-edged sword revisited. *Annu. Rev. Pathol.* **9**:119-145; 2014.

[23] Lee, M.; San Martin, A.; Valdivia, A.; Martin-Garrido, A.; Griendling, K. K. Redox-Sensitive Regulation of Myocardin-Related Transcription Factor (MRTF-A) Phosphorylation via Palladin in Vascular Smooth Muscle Cell Differentiation Marker Gene Expression. *PLoS. One.* **11**:e0153199; 2016.

[24] Martyn, K. D.; Frederick, L. M.; von Loehneysen, K.; Dinauer, M. C.; Knaus, U. G. Functional analysis of Nox4 reveals unique characteristics compared to other NADPH oxidases. *Cell Signal.* **18**:69-82; 2006.

[25] Nakano, Y.; Longo-Guess, C. M.; Bergstrom, D. E.; Nauseef, W. M.; Jones, S. M.; Banfi, B. Mutation of the Cyba gene encoding p22phox causes vestibular and immune defects in mice. *J. Clin. Invest* **118**:1176-1185; 2008.

[26] Parkos, C. A.; Allen, R. A.; Cochrane, C. G.; Jesaitis, A. J. Purified cytochrome b from human granulocyte plasma membrane is comprised of two polypeptides with relative molecular weights of 91,000 and 22,000. *J. Clin. Invest* **80**:732-742; 1987.

[27] Parkos, C. A.; Dinauer, M. C.; Jesaitis, A. J.; Orkin, S. H.; Curnutte, J. T. Absence of both the 91kD and 22kD subunits of human neutrophil cytochrome b in two genetic forms of chronic granulomatous disease. *Blood* **73**:1416-1420; 1989.

[28] Putyrski, M.; Schultz, C. Protein translocation as a tool: The current rapamycin story. *FEBS Lett.* **586**:2097-2105; 2012.

[29] Reczek, C. R.; Chandel, N. S. ROS-dependent signal transduction. *Curr. Opin. Cell Biol.* **33**:8-13; 2015.

[30] Rinchik, E. M.; Stoye, J. P.; Frankel, W. N.; Coffin, J.; Kwon, B. S.; Russell, L. B. Molecular analysis of viable spontaneous and radiation-induced albino (c)-locus mutations in the mouse. *Mutat. Res.* **286**:199-207; 1993.

[31] Schroder, K.; Zhang, M.; Benkhoff, S.; Mieth, A.; Pliquett, R.; Kosowski, J.; Kruse, C.; Luedike, P.; Michaelis, U. R.; Weissmann, N.; Dimmeler, S.; Shah, A. M.; Brandes, R. P. Nox4 is a protective reactive oxygen species generating vascular NADPH oxidase. *Circ. Res.* **110**:1217-1225; 2012.

[32] Segal, A. W. Absence of both cytochrome b-245 subunits from neutrophils in X-linked chronic granulomatous disease. *Nature* **326**:88-91; 1987.

[33] Shiose, A.; Kuroda, J.; Tsuruya, K.; Hirai, M.; Hirakata, H.; Naito, S.; Hattori, M.; Sakaki, Y.; Sumimoto, H. A novel superoxide-producing NAD(P)H oxidase in kidney. *J. Biol. Chem.* **276**:1417-1423; 2001.

[34] Sumimoto, H. Structure, regulation and evolution of Nox-family NADPH oxidases that produce reactive oxygen species. *FEBS J.* **275**:3249-3277; 2008.

[35] Sumimoto, H.; Miyano, K.; Takeya, R. Molecular composition and regulation of the Nox family NAD(P)H oxidases. *Biochem. Biophys. Res. Commun.* **338**:677-686; 2005.

[36] Ushio-Fukai, M.; Zafari, A. M.; Fukui, T.; Ishizaka, N.; Griendling, K. K. p22phox is a critical component of the superoxide-generating NADH/NADPH oxidase system and regulates angiotensin II-induced hypertrophy in vascular smooth muscle cells. *J. Biol. Chem.* **271**:23317-23321; 1996.

[37] Varnai, P.; Thyagarajan, B.; Rohacs, T.; Balla, T. Rapidly inducible changes in phosphatidylinositol 4,5-bisphosphate levels influence multiple regulatory functions of the lipid in intact living cells. *J. Cell Biol.* **175**:377-382; 2006.

[38] von Lohneysen, K.; Noack, D.; Jesaitis, A. J.; Dinauer, M. C.; Knaus, U. G. Mutational analysis reveals distinct features of the Nox4-p22 phox complex. *J. Biol. Chem.* **283**:35273-35282; 2008.

[39] von Lohneysen, K.; Noack, D.; Wood, M. R.; Friedman, J. S.; Knaus, U. G. Structural insights into Nox4 and Nox2: motifs involved in function and cellular localization. *Mol. Cell Biol.* **30**:961-975; 2010.

[40] Winterbourn, C. C. The biological chemistry of hydrogen peroxide. *Methods Enzymol.* **528**:3-25; 2013.

[41] Wu, R. F.; Ma, Z.; Liu, Z.; Terada, L. S. Nox4-derived H2O2 mediates endoplasmic reticulum signaling through local Ras activation. *Mol. Cell Biol.* **30**:3553-3568; 2010.

[42] Zhang, M.; Brewer, A. C.; Schroder, K.; Santos, C. X.; Grieve, D. J.; Wang, M.; Anilkumar, N.; Yu, B.; Dong, X.; Walker, S. J.; Brandes, R. P.; Shah, A. M. NADPH oxidase-4 mediates protection against chronic load-induced stress in mouse hearts by enhancing angiogenesis. *Proc. Natl. Acad. Sci. U. S. A* **107**:18121-18126; 2010.

LEGENDS TO FIGURES

Figure 1.

TGF-β1 stimulates H_2O_2 production in human primary dermal and pulmonary fibroblasts.

Extracellular H_2O_2 production by adherent human pulmonary (HPF, **A**) and foreskin (BJ, **B**) fibroblasts, was determined by Amplex Red assay in the presence of 50 µM Amplex Red and 0.1 U/ml horseradish peroxidase in H-medium. After 40 min incubation at 37°C, resorufin fluorescence was measured at 590 nm. HPF. Cells were treated with Nox4 or control (scrambled) siRNA for 24 h and were stimulated with 5 ng/mL TGF-β1 in serum-free medium for 24 h. Bars with SEM represent mean values of 3 independent experiments. ** P<0.001 * P<0.002 in Mann-Whitney U test or t-test.

Figure 2.

TGF-β1-stimulated H_2O_2 production by wild-type, NOX4- and $p22^{phox}$- deficient tail tip fibroblasts.

Serum-depleted, adherent, tail tip fibroblasts (TTFs) were treated with 5 ng/mL TGF-β1 for 24 h. Extracellular H_2O_2 production was measured by the Amplex Red assay in Nox4-deficient (**A**) and $p22^{phox}$– mutant cells (**B**). Bars with SEM represents mean values in 3 independent experiments. ** P<0.001, * P<0.002 in t-test

Figure 3.

$P22^{phox}$ mRNA and protein expression in primary fibroblasts and Nox4-transfected HEK293 cells

(**A**). Nox4 and $p22^{phox}$ mRNA expression levels of control and TGF-β1-induced HPFs, and BJ fibroblasts were determined after a 24 h treatment with TGF-β1. Relative expressions are expressed, where the non-induced expressions are defined as 1. (**B**). Western blot analysis of the $p22^{phox}$ protein content of control and TGF-β1-stimulated HPFs and BJ fibroblasts. (**C**). Western blot analysis of the $p22^{phox}$ protein content in lysates of Nox4-expressing and control (untransfected) HEK293 FS cells. The right panel shows the H_2O_2 output of Nox4-expressing and control cells, assessed by the Amplex Red assay. Western blot experiments yielded essentially the same result in at least three separate experiments. Mean values and SEM are calculated from 3 independent experiments* $P<0.005$ in Paired t-test. **(D).** $p22^{phox}$ protein expression of unstimulated and TGF-β1-induced TTFs, isolated from Nox4 knockout animals.

Figure 4.

Nox4 and $p22^{phox}$ expression in the kidneys of wild-type, Nox4-knockout, and $p22^{phox}$-deficient mice

(**A**-**D**) *In situ* hybridization for Nox4 and $p22^{phox}$ mRNAs in mouse kidney. (A, C: antisense probes, B, D: sense probes, PT: proximal tubule, DT: distal tubule). (**E**) Analysis of $p22^{phox}$ expression by Western blot in kidney lysates from wild-type, $p22^{phox}$ mutant (*nmf333*) and Nox4-deficient animals. (**F**) Nox4 protein detection by Western blot in kidney lysates from wild-type, $p22^{phox}$ mutant (*nmf333*) and Nox4-deficient animals.

Figure 5.

Subcellular localization of Nox4 and $p22^{phox}$ in BJ fibroblasts

Representative confocal images of permeabilized BJ cells expressing V5-tagged $p22^{phox}$ (**A**) and Nox4 (**B**) compared to endogenous BiP. Fibroblasts were transiently transfected then induced with TGF-β1 or left untreated after overnight serum depletion. The cells were fixed and immunostained with anti-V5 and anti-BiP antibody. Bars represent 10 μm.

Figure 6.

Translocation of FKBP12 domain upon heterodimerization with FRB in dermal fibroblasts.

The rapamycin-induced heterodimerization of the mammalian FRB domain with FK506 binding protein 12 (FKBP12) can be followed in confocal images. The $p22^{phox}$-FRB-CFP (**A**) or CFP-FRB-Nox4 (**B**) and YFP-linker-FKBP12 were cotransfected in BJ fibroblasts. After 24h incubation, the cells were seated in cell chamber with H-medium in the confocal microscope. Administration of 300 nM rapamycin, induced the translocalization of the FKBP12 to reach the spatially available FRB domain. Bars represent 10 μm. The schematic structure of the $p22^{phox}$ and Nox4 is shown in panels **C** and **D**.

Figure S1

Comparison of the $p22^{phox}$ content of neutrophils and primary fibroblasts

Western blot analysis of the $p22^{phox}$ protein content of different numbers of neutrophils (PMN) human pulmonary (HPF) and dermal (BJ) fibroblasts.

Figure1
Click here to download high resolution image

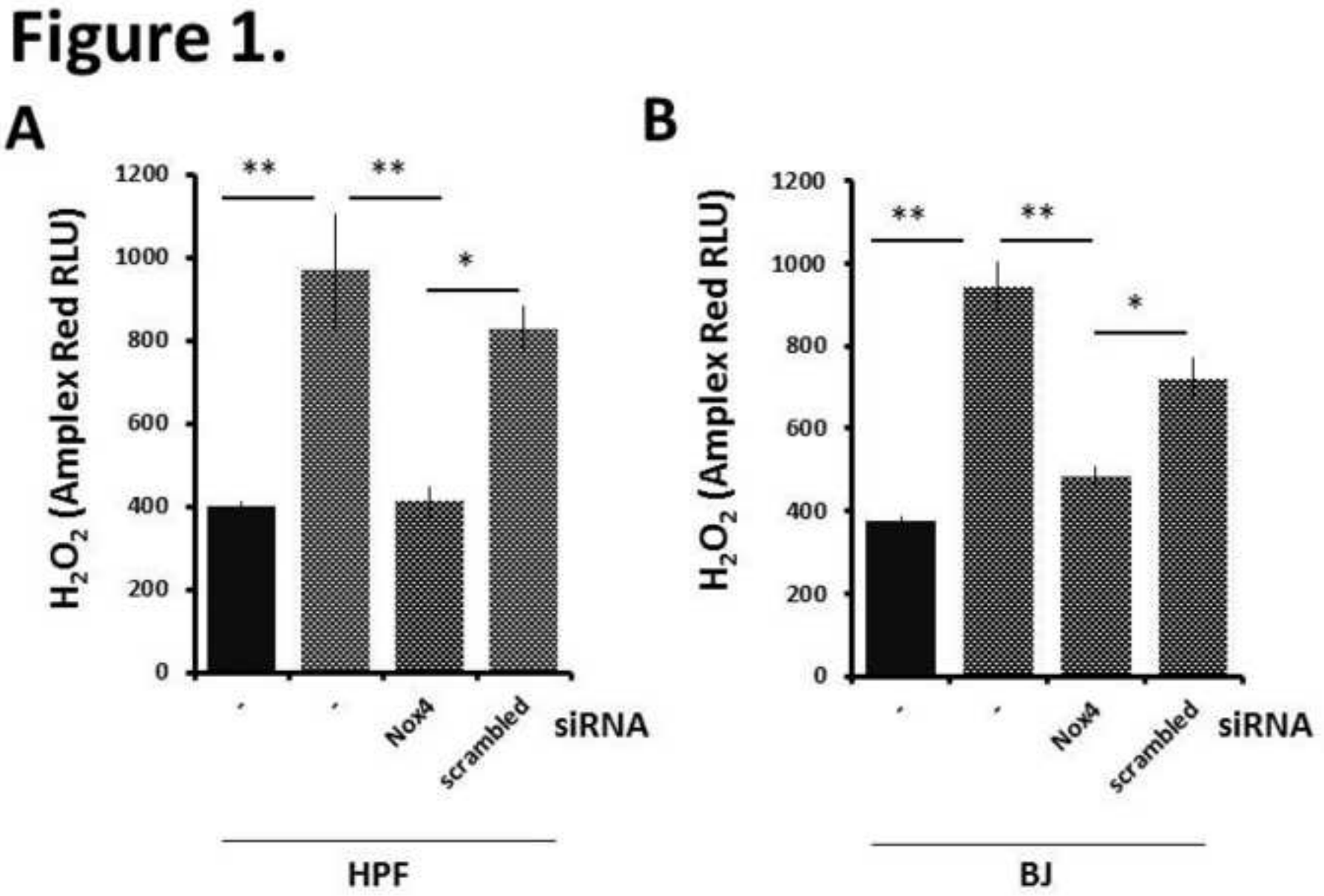

Figure2
Click here to download high resolution image

Figure 2.

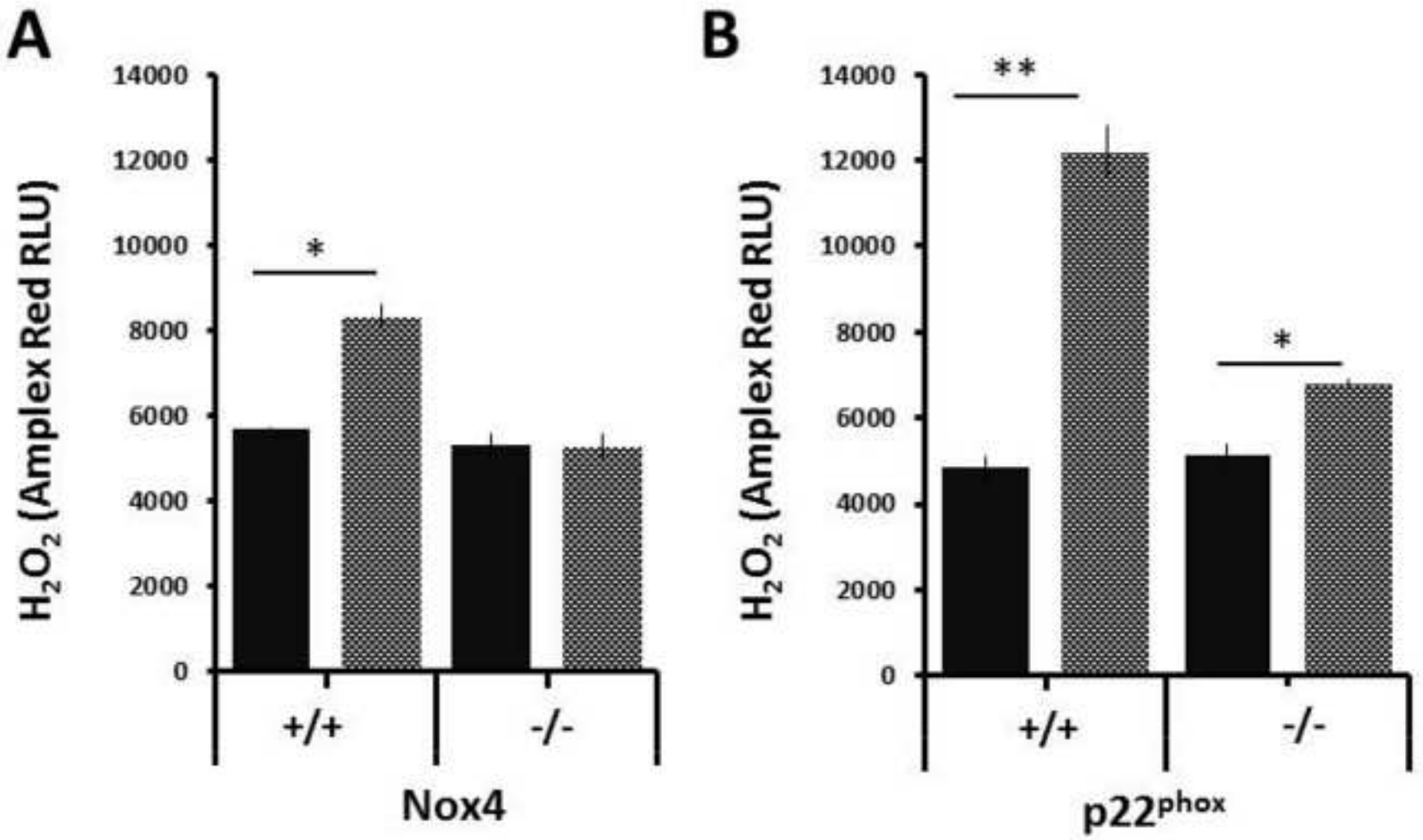

Figure3
Click here to download high resolution image

Figure 3.

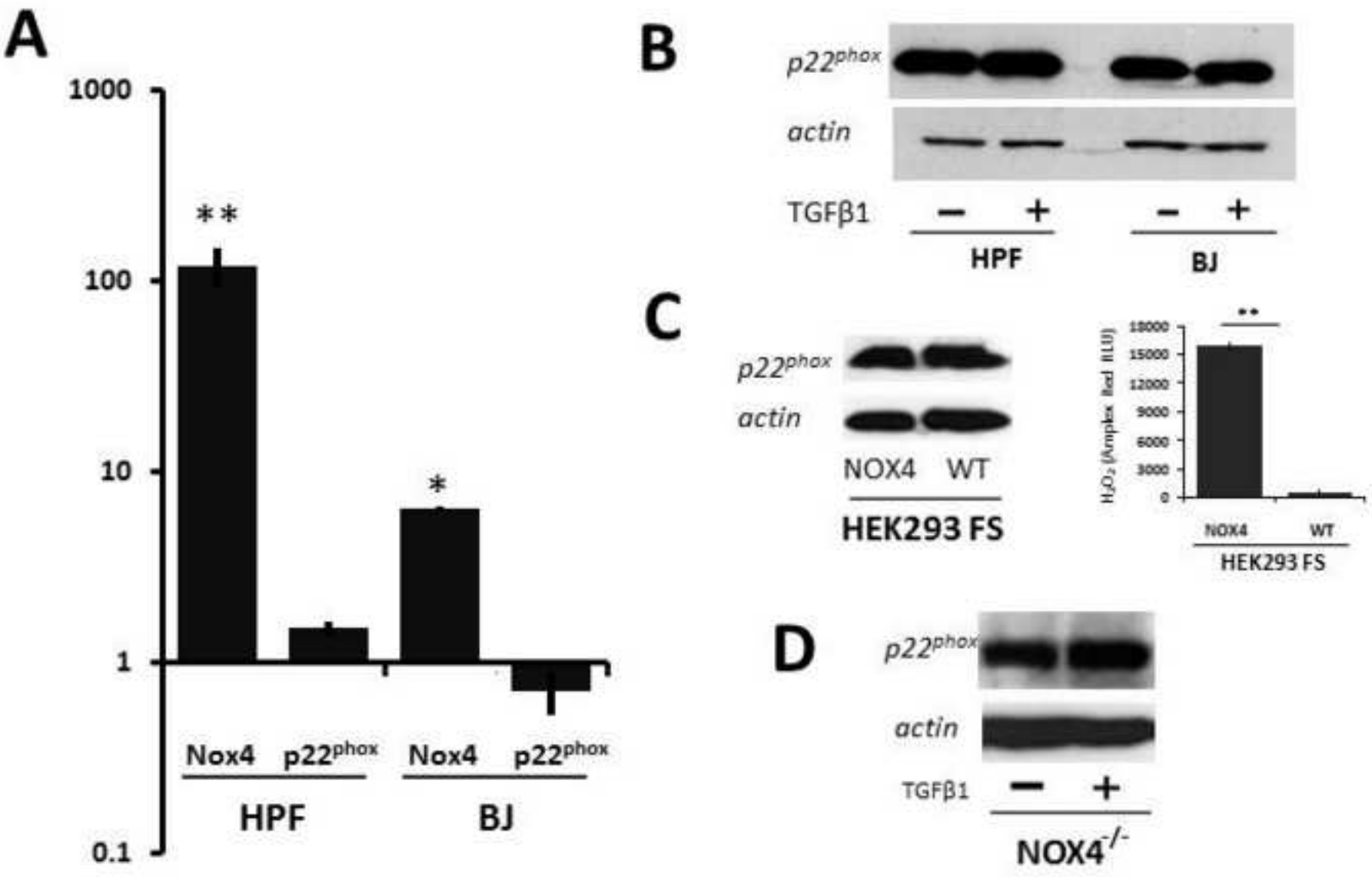

Figure4

Click here to download high resolution image

Figure 4

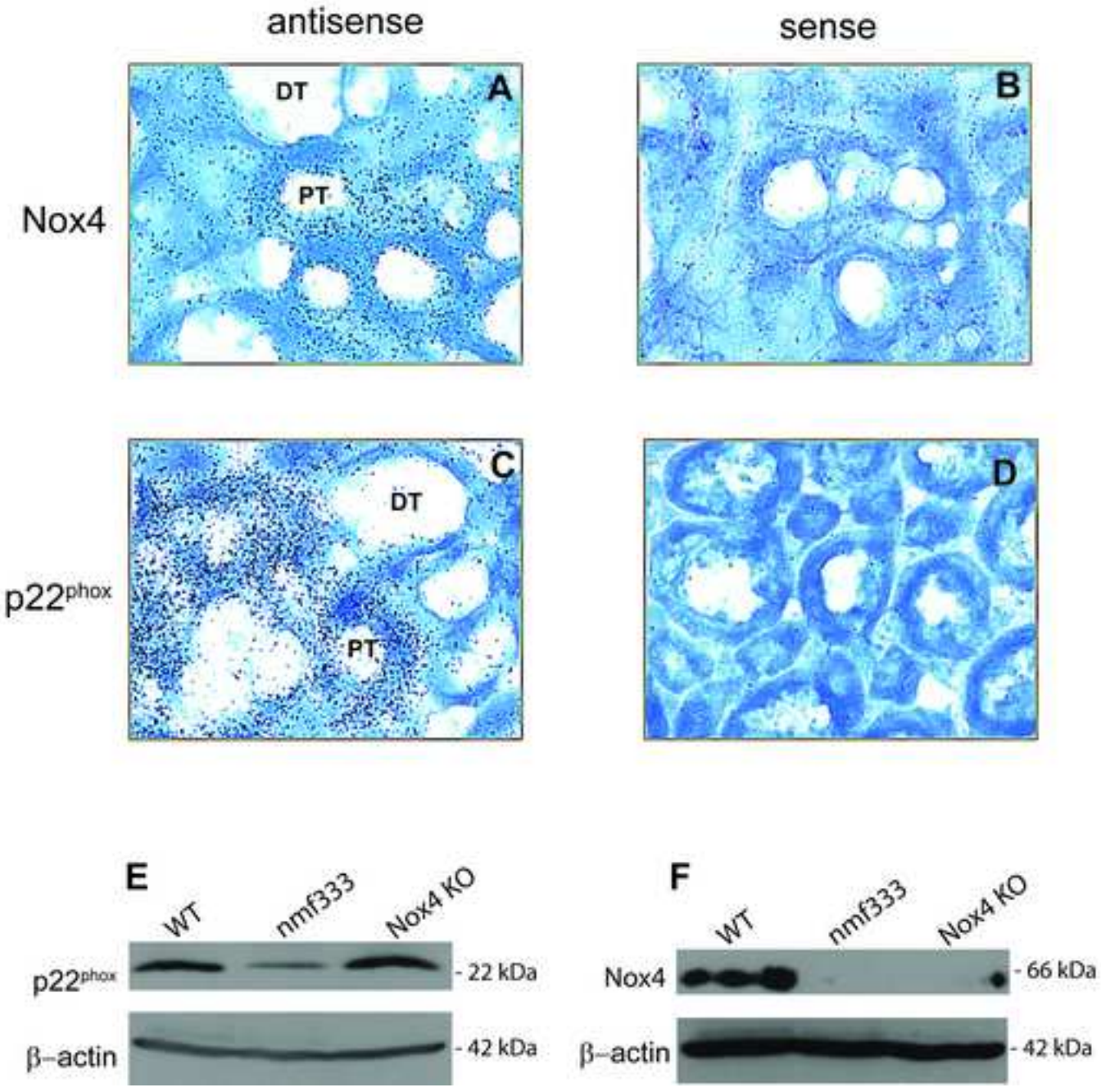

Figure5

Click here to download high resolution image

Figure 5.

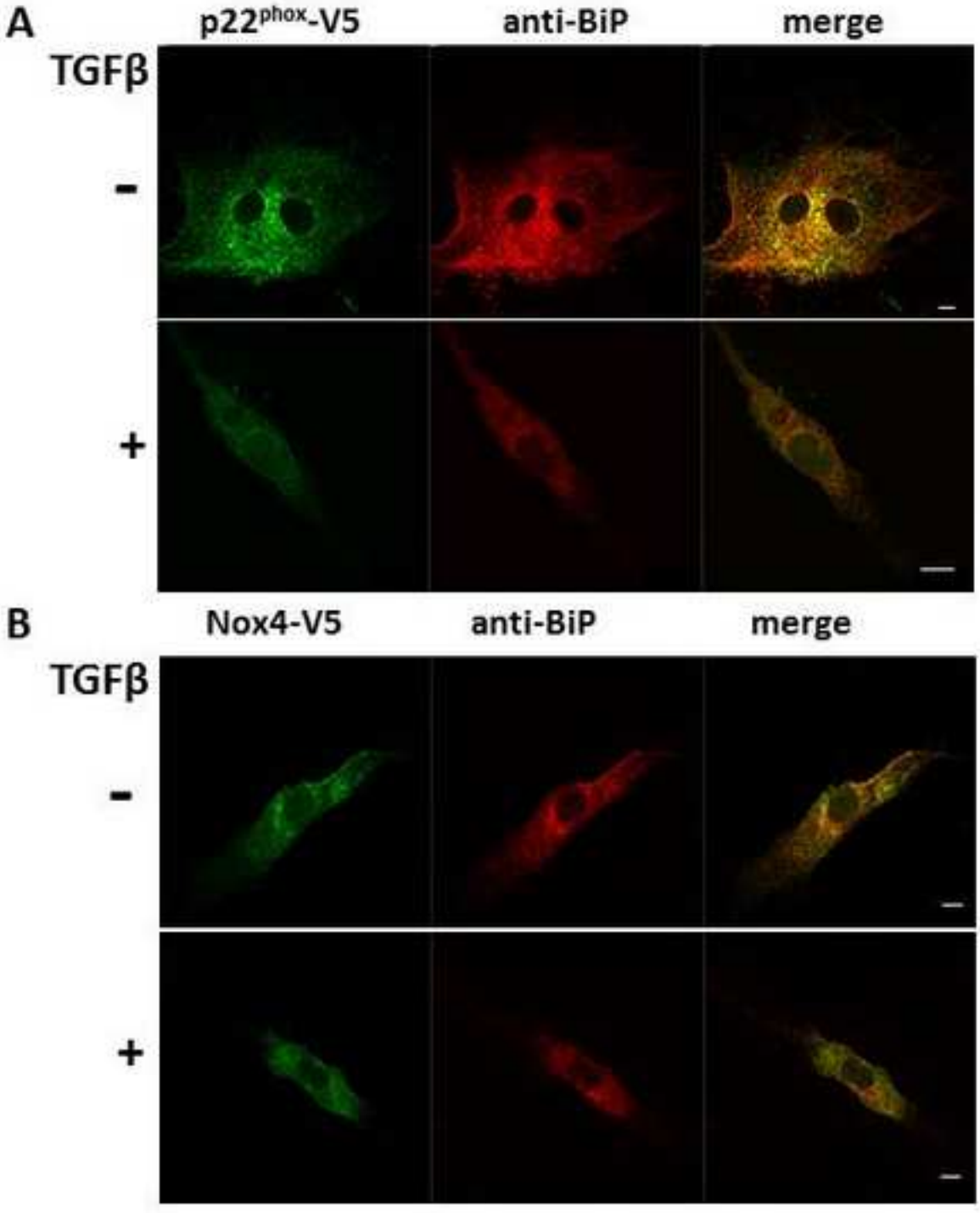

Figure6

Click here to download high resolution image

Figure 6.

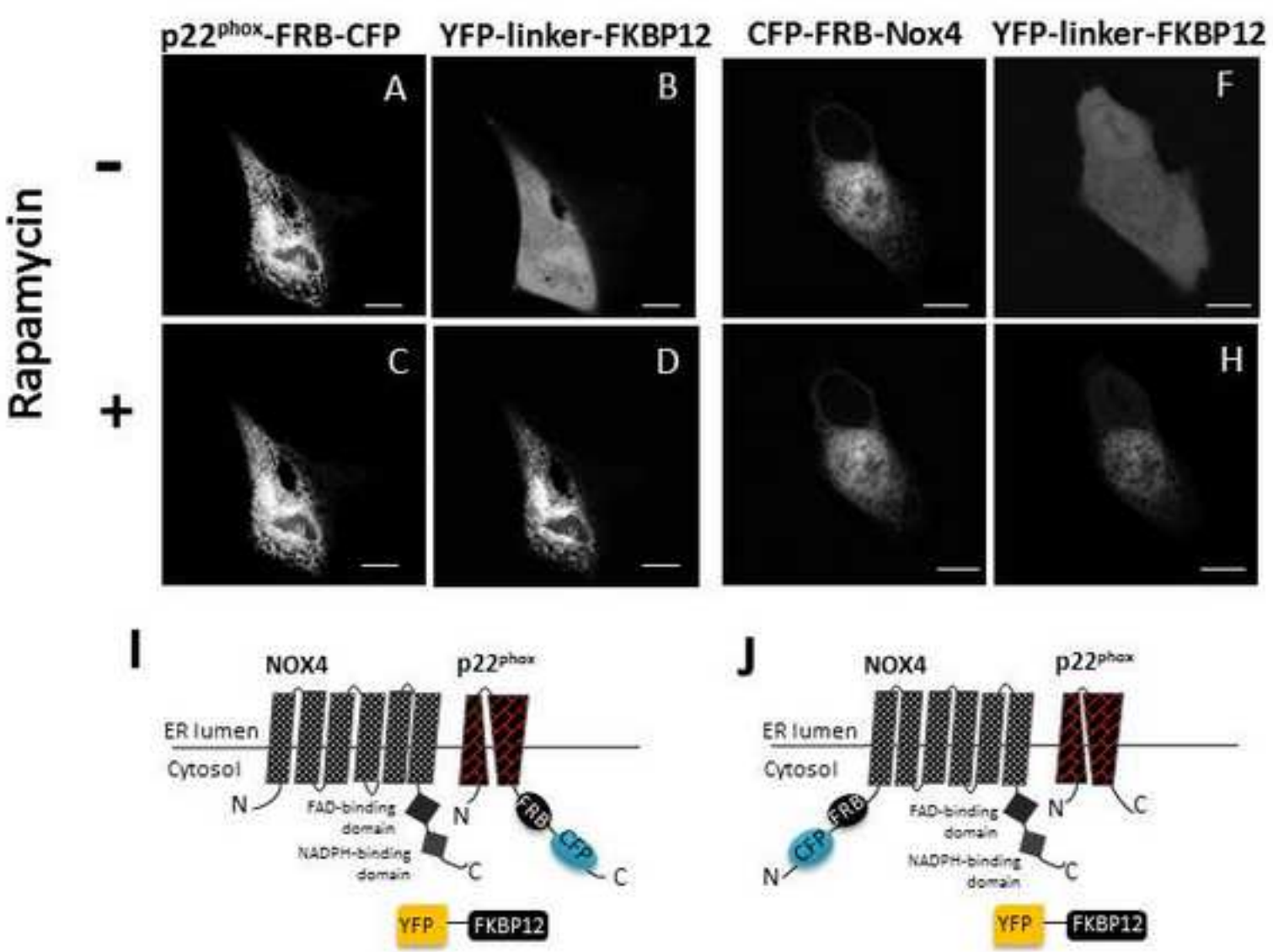

Supplementary Figure1

Click here to download high resolution image

Supplementary figure 1.